Macromolecules

ARTICLE

pubs.acs.org/Macromolecules

Biodegradable Core−Shell Materials via RAFT and ROP: Characterization and Comparison of Hyperbranched and Microgel Particles

Yu Zheng,[†] William Turner,[†] Mengmeng Zong,[†] Derek J. Irvine,[†,‡] Steven M. Howdle,[†] and Kristofer J. Thurecht*[,§]

[†]School of Chemistry and [‡]Department of Chemical and Environmental Engineering, University of Nottingham, Nottingham, U.K. NG7 2RD

[§]Australian Institute for Bioengineering and Nanotechnology and Centre for Advanced Imaging, University of Queensland, St. Lucia, Queensland 4072, Australia

Supporting Information

ABSTRACT: Two methodologies for synthesizing novel, degradable, core cross-linked copolymer particles were investigated and the molecular properties of the resultant polymers were compared. The first approach was to synthesize hyperbranched poly(ε-caprolactone-*co*-*N*,*N*-dimethylamino-2-ethyl methacrylate (PCL-*co*-PDMAEMA) by combining metal-catalyzed ring-opening polymerization (ROP) of ε-caprolactone (ε-CL) and reversible addition−fragmentation chain transfer polymerization (RAFT) of *N*,*N*-dimethylamino-2-ethyl methacrylate. First, the hyperbranched core was prepared via ROP copolymerization of ε-CL and branching agent 4,4-bioxepanyl-7,7-dione (BOD). This polymerization was initiated using the hydroxyl moiety of the bifunctional initiator 4-cyano-1-hydroxypent-4-yl dithiobenzoate (ACP-RAFT) which resulted in reactive pendent RAFT groups located on the polymer chains. The hyperbranched structure was confirmed by GPC-MALLS and NMR. Subsequent chain extension of this hyperbranched macromolecule with DMAEMA using RAFT chemistry yielded water-soluble nanoparticles. The second method involved the synthesis of core-cross-linked-shell particles (CCS) by the arm-first route. Linear arms of DMAEMA were synthesized using ACP-RAFT and subsequently used as macroinitiator for the ROP of ε-CL and BOD to form a degradable microgel that was water-soluble. Once again, molecular structure was analyzed by ^{1}H NMR, ^{13}C NMR, and GPC and molecular size by TEM. Finally, GPC-MALLS was used to qualitatively investigate the different cross-link densities of the degradable core by the two different methodologies. Thus, we demonstrate two synthetic approaches for constructing water-soluble, degradable core−shell nanoparticles that exhibit varying degrees of cross-linking by combining RAFT and ROP.

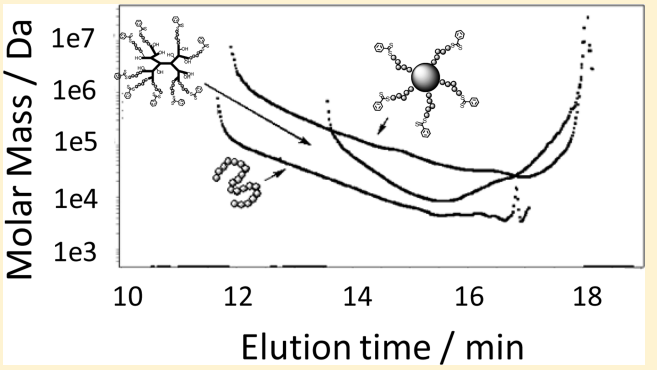

INTRODUCTION

Dendritic polymers have unique properties because of their highly branched structures and large number of functional end groups.[1,2] Their unique, three-dimensional structure also makes them attractive for new applications ranging from drug delivery to nanobuilding blocks.[2,3] Additionally, recent discoveries of new controlled polymerization mechanisms have paved the way to achievable synthetic procedures to deliver new macromolecular architectures. Hyperbranched polymers are one class of dendritic polymer that has a random branched structure. While the cost, and most certainly the synthetic challenge, of developing hyperbranched polymers is considerably lower than that of the much more structurally symmetrical dendrimer, they still exhibit many of the beneficial properties of a dendrimer. Perhaps the most important of these is the presence of a high degree of functionality both at the surface of the particle and within the branched interior.[4]

Recently, 4,4-bioxepanyl-7,7-dione (BOD) was used as a cross-linker to form a microgel or core cross-linked polymeric structure.[5,6] Both fully degradable (using ROP alone) and partially degradable (using a combination of atom-transfer radical polymerization ATRP and ROP) microgel particles were synthesized using the arm-first methodology. These microparticles had a highly dense and cross-linked, but potentially degradable, core of polycaprolactone. This is of particular importance for the design of new biomedical polymers, since discrete nanoparticles with defined size and structure could be designed which also exhibit good biocompatibility and degradability.[7]

Received: November 29, 2010
Revised: January 20, 2011
Published: February 10, 2011

Scheme 1. Scheme of Degradable Core−Shell Polymer via RAFT and ROP Route[a]

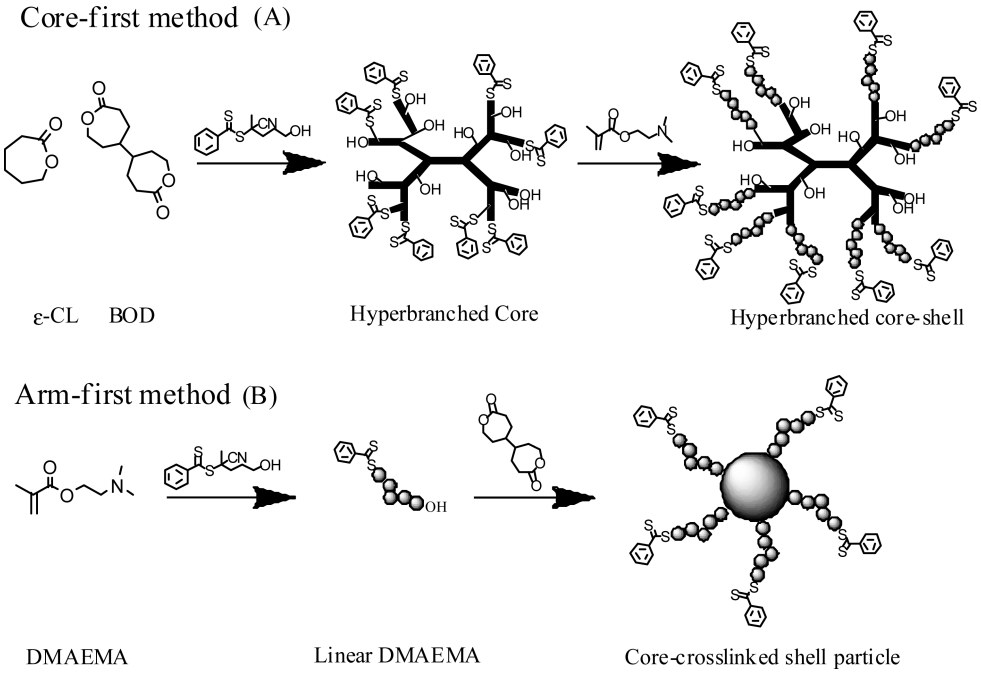

[a] Routes A and B demonstrate the core-first method (for hyperbranched particles) and arm-first method (for CCS particles), respectively.

Polyester nanoparticles have become increasingly important in the biomedical field due to the general ease of metabolization of the degradation products that are produced.[8,9] In addition, readily available feedstocks and newly developed chemistries have facilitated tuning of the polymer properties, for example, hydrophilicity and postmodification with bioligands.[7] Of equal importance is the ability to have a handle on the degree of cross-linking and hence degree of degradation and rate.

In this paper, we present a new method for the synthesis of core−shell, degradable hyperbranched polymers with varying cross-link density. The polymer consists of a hyperbranched PCL core and pH-sensitive shell. Our strategy combines the two methodologies of ROP and RAFT; an hydroxyl-group-terminated dithiobenzoate-based RAFT agent is used to initiate the ROP of lactone in the presence of a suitable catalyst, i.e., $Sn(oct_2)$, while acting efficiently as a controlling agent for methacrylate polymerization. Here, we utilize a metal-free initiator and the RAFT agent is seen as a biocompatible initiator if chosen judiciously. We compare this structure to microgel particles synthesized (so-called CCS particles) using RAFT by a modified methodology first introduced by Qiao et al.[10] The overall approach for synthesis of hyperbranched (core-first) and microgel (arm-first) degradable nanoparticles is outlined in Scheme 1. Dimethylaminoethyl methacrylate (DMAEMA) was chosen as the shell of the particles in both cases to impart solubility in aqueous solutions. The molecular conformation of the particles is investigated by SEC-MALLS which provides a qualitative comparison of cross-link density between the polymers formed by each methodology.

EXPERIMENTAL SECTION

Materials. ε-Caprolactone (ε-CL, from Aldrich, 99%) was dried over calcium hydride(CaH_2) for 48 h at room temperature and then distilled under reduced pressure before use. Bicyclohexanone was purchased from TCI Chemicals and used as received. Methyl methacrylate (MMA) and *N*, *N*-dimethylamino-2-ethyl methacrylate (DMAEMA, from Aldrich, 99%) were passed through a column of basic alumina to remove stabilizing agents and then stored under a nitrogen atmosphere at −20 °C. Toluene (Aldrich, reagent grade) and tetrahydrofuran (THF) were dried by molecular sieves before use. 4-Cyano-1-hydroxypent-4-yl dithiobenzoate (ACP-RAFT) was synthesized as previously described in the literature.[11]

Synthesis of 4,4-Bioxepanyl-7,7-dione (BOD). BOD was synthesized as previously reported.[10] Typically, a solution of urea hydrogen peroxide ($CO(NH_2)_2 \cdot H_2O_2$) (10.0 g, 106 mmol) in 50 mL of formic acid (99%) was stirred at 23 °C for 90 min. 4,4-Bicyclohexanone (5.0 g, 25.7 mmol) was then slowly added over 5−10 min and stirred for a further 4 h. 200 mL of water was added to the mixture followed by extraction with chloroform. The organic fractions were collected, washed with a saturated aqueous sodium bicarbonate solution, and dried with Na_2SO_4. The organic fraction was concentrated, and the solvent was removed under reduced pressure to yield a white powder (3.50 g, 60% yield). ^{1}H NMR (300 MHz, $CDCl_3$): 4.34 (R, R) 4.17 (S, R) (t, 2H, $-CH_2-$ OOC−), 2.73 (R, R) 2.60 (S, R) (t, 2H, $-CH_2COO-$), 1.93−1.83 (m, 2H, $-CH_2CH_2OOC-$), 1.70−1.60 (m, 2H,-CH_2CH_2COO-), 1.49 (q, 1H, $-CHCH_2-$).

Synthesis of ACP-RAFT-Functional Hyperbranched Poly(CL-*co*-BOD). A three-neck round-bottomed flask equipped with a rubber septum, three-way tap, and condenser were flame-dried. BOD (475 mg, 2.1×10^{-3} mol), ACP-RAFT (554 mg, 2.1×10^{-3} mol), and ε-caprolactone (2.42 g, 2.1×10^{-2} mol) were added to 50 mL of dried toluene. Stannous octanoate ($Sn(Oct)_2$) (405 mg, 1×10^{-3} mol) was added to the flask and then heated to 110 °C. The ratio [ACP-RAFT]:[BOD]:[ε-caprolactone]:[$Sn(Oct)_2$] was 1:1:10:0.5. After the desired reaction time, a 10 mL sample was withdrawn, and the polymer was then selectively precipitated in an excess volume of cold methanol, filtrated, and dried under reduced pressure.

Synthesis of Hyperbranched Core−Shell Poly(CL-*co*-BOD)$_{core}$−(DMAEMA)$_{shell}$ via RAFT. Poly(CL-*co*-BOD) (1.5 g, 1×10^{-4} mol) and ACP initiator (7.8 mg, 3.46×10^{-5} mol) were put in a dry round-bottomed flask. DMAEMA (13.6 g, 8.65×10^{-2} mol) in dry toluene (170 mL) was injected into the reaction vessel, and the system

was freeze−pump−thawed three times to remove oxygen. Assuming there are an average of 17.3 [ACP-RAFT] sites on each poly(CL-*co*-BOD) core (see eq 2), the amount of ACP-RAFT sites in the reaction mixture was 1.73×10^{-3} mol. Thus, the chemical ratio [ACP-RAFT sites]:[DMAEMA]:[ACP initiator] was 1:50:0.2 with an overall DMAEMA concentration of 0.5 M. The solution was heated to 65 °C and allowed to react for 12 h. The polymer was precipitated in excess cold hexane and dried in a vacuum oven.

Degradation of Poly(PCL-*co*-BOD)$_{core}$−(DMAEMA)$_{shell}$ Hydrolyzable Core. Dioxane (18 mL, 2.04×10^{-4} mol), hydrochloric acid (1.5 mL, 30%) and poly(PCL-*co*-BOD)$_{core}$−(DMAEMA)$_{shell}$ were mixed in a flask; the solution was heated to 60 °C and stirred for 24 h. After neutralization by NaOH and extraction, a fine pale yellow powder was collected and analyzed by NMR and GPC.

Synthesis of Arm-First CCS DMAEMA-*co*-BOD. Linear DMAEMA with a target molecular weight of 6 kDa (at 100% conversion) was synthesized using ACP-RAFT as controlling agent at 65 °C. The isolated and purified polymer (M_n = 4.7 kDa, PDI = 1.3, 79% conversion) was used as the arms for the synthesis of CCS particles. 0.5 g of polymer (1.06×10^{-4} mol) and 130 mg of BOD (6.28×10^{-4} mol) were dissolved in dry toluene (20 mL) in a 100 mL round-bottomed flask, followed by the addition of 25 mg of $Sn(Oct)_2$ (6.28×10^{-5} mol). The flask was then backfilled with argon and immersed in an oil bath at 110 °C for 24 h. The solution was then precipitated into cold hexane with the precipitate being collected by filtration and dried overnight under vacuum.

The pure degradable CCS particle used in conformational analysis was synthesized as previously described in the literature.[12]

Gel Permeation Chromatography (GPC). *Hyperbranched Polymer.* Number-average molecular weight (M_n), weight-average molecular weight (M_w), and dispersity (M_w/M_n) were obtained by gel permeation chromatography (PL-120, Polymer Laboratories) with an RI detector. The columns (30 cm PLgel Mixed-C, 2 in series) were eluted by THF and calibrated with polystyrene standards. All calibrations and analyses were performed at 40 °C and a flow rate of 1 mL/min. All of the products easily dissolved in THF and passed through a 0.2 μm filter before injection with little or no backpressure observed—demonstrating the absence of macrogelation.

CCS Polymer. GPC was performed using a Waters 333 system fitted with an RI detector. Two Styragel HT3 columns were attached in series and eluted with DMF at a flow rate of 1 mL/min at 40 °C. As with the hyperbranched polymers, the polymer was dissolved in solvent to 5 mg/mL and passed through a 0.2 μm filter before analysis.

A Dawn 8-angle MALLS detector from Wyatt Technologies was used for light scattering experiments in both solvents. The Astra software package for Windows was used to process the data.

NMR Analysis of the Polymers. ^{1}H was carried out on a 300 MHz Bruker spectrometer with MestRec processing software. The chemical shifts were referenced to the residual solvent $CHCl_3$. ^{13}C experiments were carried out in the solid state using a Bruker Avance III 300 spectrometer. Solid samples were spun to ~5 kHz in a MAS probe equipped with double-air bearings. The ^{13}C NMR spectra were recorded using a CP pulse sequence with contact time of 2 ms, a recycle delay of 3 s, and typically 2000 scans were sufficient to obtain very good signal-to-noise. The spectra were calibrated to adamantane at 38.22 ppm.

Particle Size Determination. The size distribution of hyperbranched and CCS PCL-*co*-DMAEMA was measured using dynamic light scattering on a Zetasizer nano series (Malvern Instruments Ltd.). After being filtered through a 0.2 μm filter, the samples were measured at a temperature of 25 °C. The errors in the measurements of the molecular size from DLS are within 5% of the mean value for 10 experiments over a cumulative time of 1 min per experiment. Transmission electron microscopy (TEM) was also used to investigate the size of the CCS particles. PCL-*co*-DMAEMA CCS particles were dissolved in THF to a concentration of 50 μg/mL. 100 μL of solution was dropped on a holey carbon grid and left to dry for 30 min. The TEM micrograph was measured using a JEOL JEM-200 FXII electron microscope operating at 200 keV.

Table 1. Polymerization Data for the Synthesis of Hyperbranched Poly(CL-*co*-BOD)[a]

entry	reaction time/h	M_n/kDa	M_w/kDa	PDI	d*n*/d*c* (mL/g)	conversion/%
1	1	6.4	11.3	1.76	0.082	21
2	2	11.5	15.0	1.3	0.08	40

[a] M_n, M_w, and PDI are determined by gel permeation chromatography equipped with MALLS detector. Yield of ε-caprolactone-*co*-BOD is calculated gravimetrically.

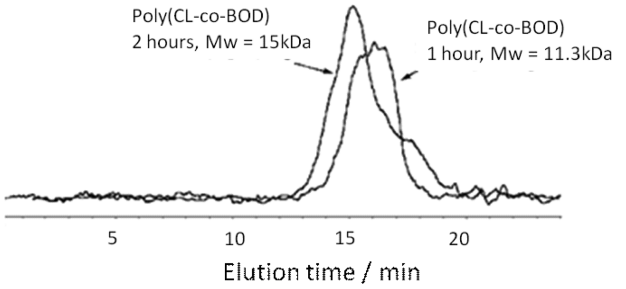

Figure 1. MALLS traces showing molecular weight evolution of hyperbranched poly(CL-*co*-BOD) with time. A clear shift to higher molar mass is observed from 1 to 2 h.

RESULTS AND DISCUSSION

Core−Shell Hyperbranched Poly(CL-*co*-BOD)$_{core}$−DMAEMA$_{shell}$. In this work, hyperbranched core−shell poly(CL-*co*-BOD)$_{core}$−DMAEMA$_{shell}$ polymers were synthesized via a two-step process involving the synthesis of hyperbranched degradable poly(CL-*co*-BOD) core via ring-opening polymerization, followed by chain extension with DMAEMA via RAFT to give the shell.

In the first step, ring-opening copolymerization of ε-caprolactone and 4,4-bioxepanyl-7,7-dione (BOD) was performed in the presence of a catalyst (stannous 2-ethylhexanoate) and an initiator (ACP-RAFT) in toluene ([CL] = 0.42 M, 110 °C) to produce an organic solvent-soluble hyperbranched poly(CL-*co*-BOD) core with pendant RAFT groups. The reaction was followed over 2 h, and the molecular weight characteristics and gravimetric yield are presented in Table 1. It was noted that macrogelation occurred once conversion increased beyond 40%. While the synthesis of hyperbranched polymers by this method using free-radical chemistry has been reported and recently reviewed,[4] to our knowledge this is the first instance of hyperbranched PCL being synthesized by this approach.

Table 1 shows that conversion reaches 40% after 2 h. As suggested previously in reports on free-radical approaches to hyperbranched polymers, the key to typically avoiding macrogelation is to prevent the ratio of [initiator]:[cross-linker] from exceeding 1.[1,13−2321] Thus, the ratio of [ACP-RAFT]:[BOD]:[ε-caprolactone] in this work is kept at 1:1:10 so as to provide a hyperbranched poly(CL-*co*-BOD) core. The relatively low ratio of monofunctional:difunctional monomer was used in order to obtain highly branched molecules, and this typically necessitated termination of the polymerization at low conversion (<50%) in order to prevent macrogelation. The GPC-MALLS traces (Figure 1) for the synthesis of hyperbranched poly(CL-*co*-BOD) clearly show the

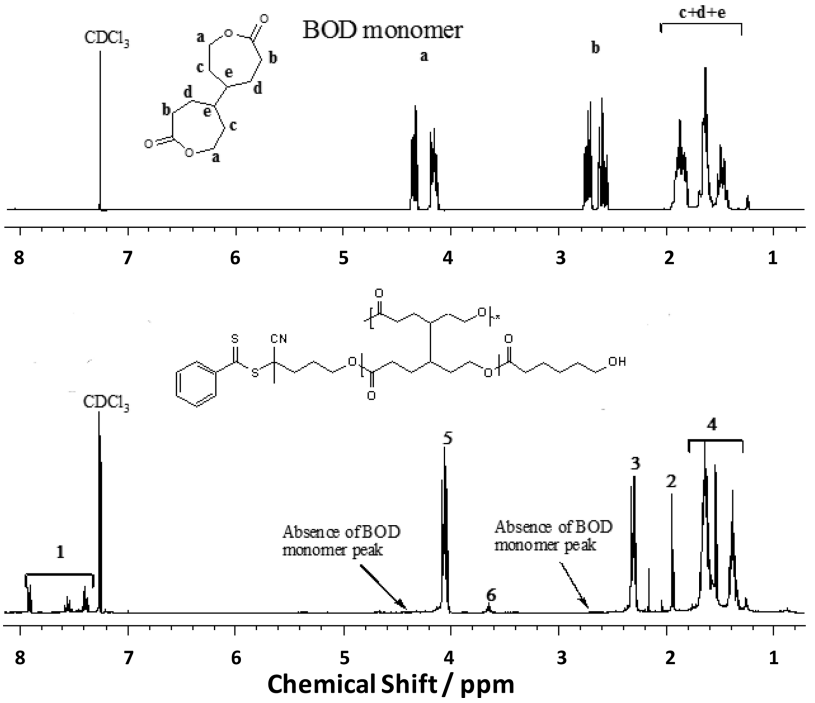

Figure 2. ^{1}H NMR spectrum of hyperbranched poly(CL-*co*-BOD) measured in $CDCl_3$ (entry 2, Table 1). The peaks due to ACP-RAFT initiator (peaks 1 and 2) and ε-caprolactone units (or BOD units, peaks 3−6) are evident in the polymer spectrum.

molecular weight evolution of the hyperbranched polymer as a function of time. As the reaction proceeds from 21% conversion to 40% conversion, the GPC peak shifts to shorter retention time (higher molecular weight) and a multimodal peak is observed as is typical for hyperbranched polymers and signifies an increase in branching.

The molecular structure of hyperbranched poly(CL-*co*-BOD) was confirmed by ^{1}H NMR (Figure 2b; Table 1, entry 2). The peaks due to the ACP-RAFT end-groups (peaks 1 and 2), ε-caprolactone, and BOD units (peaks 3−6) in the polymer are clearly discernible. In addition, the NMR spectrum shows that the peaks due to residual BOD monomer are negligible. This indicates that there are very few pendant, unreacted BOD rings remaining in the hyperbranched poly(CL-*co*-BOD) core upon purification. It should be noted that peaks due to polyBOD or polyPCL are indistinguishable in the ^{1}H spectrum as has been previously published.[12] The ^{1}H NMR spectrum of BOD is shown for comparison (Figure 2a).

The clear presence of the phenyl protons from the dithiobenzoate of the RAFT (at 7.4−7.9 ppm) and the methylene protons adjacent to the terminal hydroxyl groups (at 3.6 ppm) and the fact that both rings of the BOD appear to have been opened suggest that the composition of the hyperbranched polymer can be calculated by following equation (eq 1):

$$\frac{\text{RAFT end group}}{\varepsilon\text{-CL} + \text{BOD}} = \frac{(\text{integrals of peak 1})/5}{\left(\text{integrals of peak 5} - \dfrac{\text{integrals of peak 1}}{2/5}\right)/2} = 0.19 \quad (1)$$

The result shows that the ratio of RAFT end groups to ε-caprolactone plus BOD is equal to 1:5.2. Assuming instantaneous initiation of the RAFT hydroxyl groups, this is just higher than that expected from the feed ratio of RAFT to ε-caprolactone and BOD at 40% conversion; this was approximately 1 to 4. On the basis of the feed ratio of initiator to monomers, the number of initiators should be equal to the branching points—so at 40% conversion, one BOD unit and one initiator per 4.2 ε-caprolactone units. The assumption is also made that the RAFT agent is an efficient initiator, and all chains are initiated by the hydroxyl group on the RAFT agent.[24−26] If these assumptions hold, then the number of RAFT end-groups per polymer can be calculated based on the molecular weight measured by an absolute GPC method (e.g., MALLS). Thus, at 40% conversion, there are on average 11.8 ACP-RAFT end-groups in one hyperbranched poly(CL-*co*-BOD).

Using the core material that had a weight-average molecular weight of 15 kDa (entry 2, Table 1; entry 1, Table 2), the polymer was reacted with DMAEMA to chain extend the living RAFT end-groups. This polymerization was conducted under typical RAFT conditions in toluene at 65 °C, and 42% conversion of DMAEMA monomer was achieved after 12 h (as determined gravimetrically). Table 2 lists the polymerization data for this reaction (entry 2, Table 2), and ^{1}H NMR of the purified product was used to confirm the structure (Figure S1, Supporting Information). Assuming that there are ∼11.8 RAFT sites per hyperbranched molecule, the ratio of RAFT sites, initiator, and monomer in the feed is kept at [ACP-RAFT sites]:[DMAEMA]:[ACP initiator] = 1:50:0.2. After 12 h, the poly(CL-*co*-BOD)$_{core}$−DMAEMA$_{shell}$ is formed, and the M_n is shown to have increased to 38 kDa as measured by GPC-MALLS (entry 2, Table 2). In addition, the GPC chromatograms from the RI detector (Figure 3) show the molecular weight evolution during this chain extension. The GPC trace clearly shows the polymer peaks shifted to higher molecular weight and became broader upon chain extension with DMAEMA.

Since the hyperbranched poly(CL-*co*-BOD) core was formed by random coupling of various numbers of primary chains, the

dx.doi.org/10.1021/ma1027092 |*Macromolecules* 2011, 44, 1347–1354

Table 2. Chain Extension Polymerization Data for the Synthesis of Core−Shell Poly(CL-*co*-BOD)−(DMAEMA) and Subsequent Hydrolysis

entry	reaction time/h	M_n/kDa[a]	M_w/kDa[a]	PDI	d*n*/d*c*
1. PCL-*co*-BOD$_{core}$	0[b]	11.5	15.0	1.3	0.08
2. PCL-*co*-BOD$_{core}$−DMAEMA$_{shell}$	12[c]	38.3	68.6	1.8	0.142
3. hydrolyzed product	NA	3.1	3.9	1.2	0.169

[a] M_n and M_w are calculated by GPC-MALLS. [b] This entry is for the poly(CL-*co*-BOD) core, the same as entry 2, Table 1. [c] Yield of DMAEMA chain extension determined gravimetrically (41%).

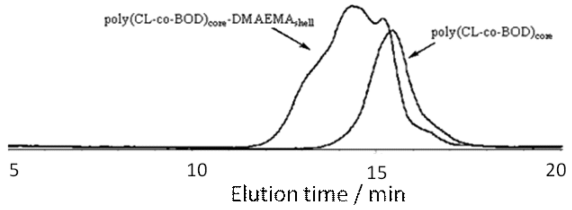

Figure 3. GPC trace using RI detector for chain extension from poly(CL-*co*-BOD)$_{core}$−DMAEMA. The GPC trace shows the evolution of molecular weight following chain extension with DMAEMA and subsequent broadening of the molecular weight distribution.

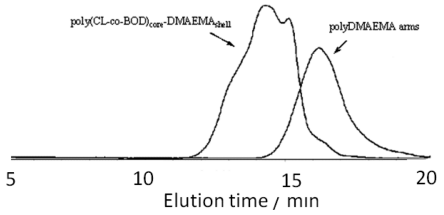

Figure 4. GPC trace of core−shell poly(CL-*co*-BOD)−DMAEMA (Table 2, entry 2) before and after (Table 2, entry 3) hydrolysis. The clean shift to lower molecular weight upon hydrolysis clearly demonstrates that degradation of the core has occurred.

number of actual initiating sites per core is unknown although it has been theoretically estimated to be 11.8 to allow the calculation of the molar ratio for the chain extension experiments. In order to determine the average number of arms per molecule (N_{arm}) for hyperbranched polymers, it is necessary to determine the length or M_n of a typical PDMAEMA arm. Thus, the PCL core was degraded under acidic conditions, and the remaining polymer was analyzed by GPC (GPC trace from RI detector shown in Figure 4).

Following hydrolysis, the molecular weight of the remaining polymer was determined by GPC-MALLS and found to be 3.1 kDa. Therefore, the average number of DMAEMA arms per core−shell molecule can be calculated based on eq 2:

$$N_{av}\ \text{armsperpolymer} = \frac{(\text{total } M_n) - (\text{core } M_n)}{\text{arms } M_n} \qquad (2)$$

Once again, if we assume that the number of ACP-RAFT groups present in each molecule is equal to the feed ratio as described above, then 8.6 (73%) RAFT end-groups on the poly(CL-*co*-BOD) have been chain extended with DMAEMA. The remaining 27% of RAFT functionalities are inactive, presumably buried within the highly branched molecule and inaccessible to chain extension. This result was also confirmed by ^{1}H NMR whereby the degree of polymerization of the

Table 3. Polymerization Data for the Synthesis of Core Cross-Linked Core−Shell PolyMMA-*co*-BOD

entry	reaction time/h	M_n/ kDa[a]	M_w/ kDa[a]	PDI	yield[b]
1. PDMAEMA	10	4.7	6.2	1.3	71
2. PDMAEMA-*co*-BOD$_{CCS}$	4	29.1	44.5	1.5	15
3. PDMAEMA-*co*-BOD$_{CCS}$	8	44.2	69.3	1.6	26
4. PDMAEMA-*co*-BOD$_{CCS}$	24	48.7	130.2	2.6	48

[a] M_n and M_w are calculated by GPC-MALLS using DMF as eluent at 40 °C. [b] Yield determined gravimetrically.

DMAEMA was determined to be 18.5 by integration of the phenyl protons of the RAFT agent (~7.6 ppm) and the methylene protons of DMAEMA (2.6 ppm, Supporting Information Figure S1). On the basis of the molar masses measured by GPC-MALLS, the number of ACP-RAFT groups that were chain extended was determined to be 9.2—this closely matches the theoretical value described above.

The removal of the poly(CL-*co*-BOD) core from the core−shell polymer after hydrolysis was also confirmed by NMR analysis (Figure S1b, Supporting Information). In the spectrum of the core−shell polymer, the peaks at 1.40, 1.65, and 2.30 ppm (all assigned to the poly(CL-*co*-BOD) core[27,28]) are no longer present upon hydrolysis, suggesting that the hydrolysis reaction was successful.

Arm-First Core−Shell PCL-*co*-PDMAEMA. The second method of forming degradable core−shell particles was by using the arm first approach. This technique involved the synthesis of microgel particles that were stabilized by presynthesized polymeric arms.[17,29] Unlike the hyperbranched procedure, the degradable cores of the CCS particles are synthesized using 100% cross-linker (BOD); macrogelation of the system is minimized by a combination of dilution effects and stabilization of the particles using linear polymer arms. This approach has been previously discussed in the literature using ring-opening polymerization.[6,10,12] PDMAEMA was chosen as a representative polymer for the arms of the microgels, and low-molecular-weight polymers were synthesized using ACP-RAFT. The oligomer obtained showed relatively narrow PDI (Table 3, entry 1).

Utilization of PDMAEMA allows the formation of a CCS particle with nondegradable arms and a fully degradable core and should impart water solubility onto the particle; to our knowledge, synthesis of such particles using RAFT has not been reported. The microgel reaction was monitored by GPC (Table 3, entries 2−4), and progression to higher molecular weight was clearly observed with increasing reaction time. The initial trace (Figure 5, DMAEMA arms) relates to an aliquot removed from the reaction immediately after the injection of BOD; this peak is not present (or low concentration) in the final

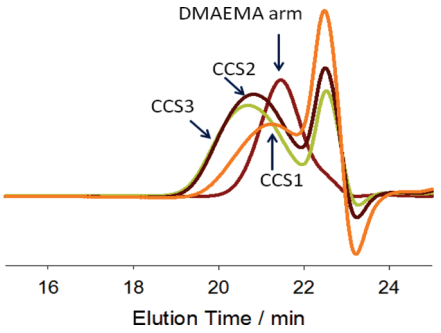

Figure 5. RI GPC trace in DMF of DMAEMA arms and CCS particles as a function of reaction time (Table 1, entries 1−4).

CCS particle after 24 h reaction (Figure 5), indicating that essentially all of the DMAEMA arms have been involved in the stabilization of the CCS particles.

The progression toward higher molecular weights was monitored after 4, 8, and 24 h. The final sample (removed 24 h after the injection of BOD) displays a large and broad peak at short retention time correlating to the CCS particles. ^{1}H NMR was used to monitor the composition of the CCS particle (Figure 6), and the structure was confirmed using solid-state ^{13}C NMR (Figure S2, Supporting Information). The peaks corresponding to the DMAEMA and PCL constituents from ^{1}H NMR are assigned in Figure 6. Importantly, the aromatic peaks at 7.3−7.8 ppm belonging to the pendant RAFT dithiobenzoate groups clearly show that the RAFT agent is present on the macromolecules. Likewise, the methylene groups adjacent to hydroxyl end-groups are also present at 3.65 ppm. Similarly, the methylene groups immediately adjacent to the amino groups in DMAEMA (2.6 ppm) are clearly well-separated from other peaks in the spectrum and prove the presence of the PDMAEMA chains in the copolymer.

The number of arms per CCS particle was estimated from the GPC-MALLS data as outlined in the hyperbranched section above. Assuming that all PDMAEMA-RAFT chains initiated the ROP of BOD and knowing the feed composition, at 49% conversion the number-average of arms per CCS particle was calculated to be 9.5.

Size Analysis of PMMA-BOD CCS Particles. One advantage of CCS and hyperbranched nanoparticles is that they are intrinsically shape-persistent due to the high level of cross-linking in the core. This is in contrast to micellar systems that require solvent selectivity for a particular moiety to form a micelle above the critical micelle concentration (cmc). This shape-persistent character of these particles facilitates a wide range of size analyses. TEM and DLS were used as two complementary methods of characterizing the size of the CCS particles—DLS in solution and TEM upon drying following deposition on a grid. Figure 7 shows the DLS and TEM results for entry 4 of Table 3 using THF as solvent. Here, the particle size distribution maximum is at 8 nm, and the sizes cover the range from 5 to 15 nm. There also exists a size distribution at around 50−60 nm, which we attribute to particle agglomeration in the solvent. A TEM micrograph is also shown in Figure 7 following deposition of the polymer from THF directly onto a TEM grid. The image shows agglomerated regions of sphere-like particles in the size range of 10−15 nm. Unfortunately, because of concentration effects during the drying process, the particles tend to agglomerate on the grid during evaporation of the solvent. Nonetheless, the TEM size range of

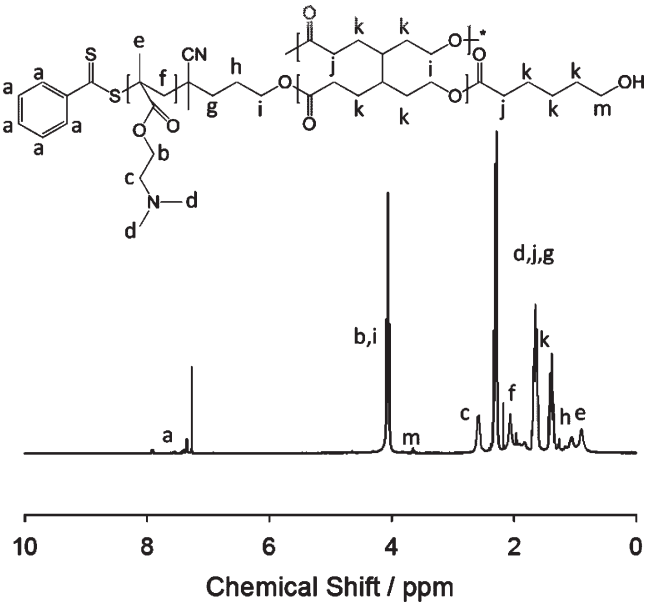

Figure 6. ^{1}H NMR spectrum of DMAEMA-BOD CCS in $CDCl_3$. Note that RAFT (peak a: phenyl groups in dithiobenzoate) and hydroxyl (peak m: methylene adjacent to hydroxyl) end-groups are present in the spectrum.

the particles is similar to the results calculated from DLS. Particles within the size range of 5−10 nm fall within the expected range for molecules having such a molecular weight with a densely packed core.

Comparison of Molecular Structure of Hyperbranched and CCS Degradable Particles. The cross-link density of the degradable segment in nanoparticles for biomedical applications can play a very important role in the degradation rate and mechanism.[30] Thus, it is important to distinguish, at least qualitatively, any conformational differences between hyperbranched poly(CL-*co*-BOD), linear PCL, and cross-linked core star (CCS) PCL. Purely degradable hyperbranched and CCS polymers were used in this comparison to minimize errors due to refractive index differences in the respective copolymers and hence yield a relationship directly related to cross-link density (rather than molecular effects). Linear PCL was prepared using ACP-RAFT as initiator and core-star particles (both CCS and hyperbranched) using linear PCL arms initiated using ACP-RAFT. Thus, the polymer end-groups were the same in all molecules. Comparison of the plots of molecular weight against elution volume between structurally different species can reveal differences in the behavior of these molecular structures, since SEC elution time is directly related to the hydrodynamic radius of the polymer in solution (not necessarily the molecular size).

Figure 8 compares the log M_w (as calculated using an absolute molecular weight method, i.e., MALLS) versus elution time for the three species. The M_w of CCS polymer as synthesized by the arm-first method is an order of magnitude higher than linear polymer at the same elution volume. Furthermore, the molecular weight at various elution times of hyperbranched poly(CL-*co*-BOD) (entry 2, Table 1) lies between that measured for the linear PCL and CCS sample. This suggests that the CCS BOD is the most densely packed structure because it has the highest molar mass at any particular hydrodynamic radius compared to both the hyperbranched and linear polymer. This was expected because the core of this polymer was synthesized using 100%

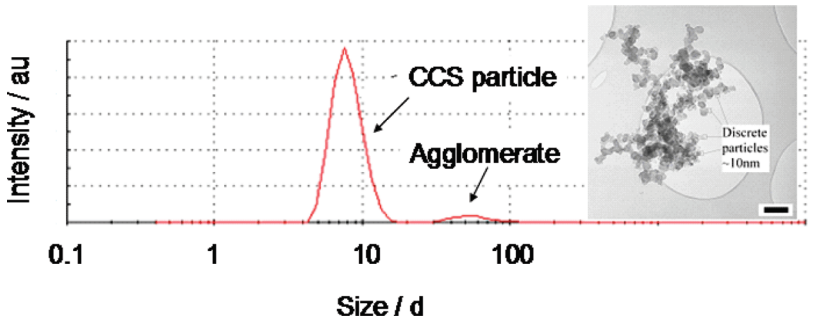

Figure 7. DLS data showing size of PMMA-BOD CCS nanoparticles in THF. TEM micrograph is included as inset showing the existence of discrete particles in the size range of 10−15 nm (scale bar is 50 nm).

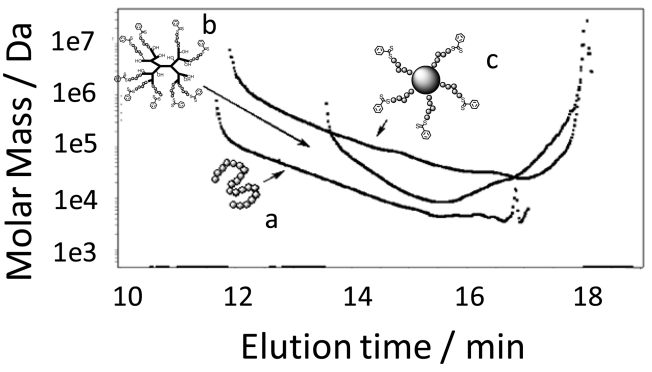

Figure 8. Plots of the log M_w versus elution volume for linear PCL (a), hyperbranched poly(CL-BOD) (b), and core cross-linked star poly-BOD (c).

cross-linker and presumably forms a microgel structure. In this latter case, the microgel core size, stability, and gelation was influenced by the presence of the PDMAEMA arms which act in a similar fashion to a traditional dispersant. The hyperbranched species is less densely packed than the CCS, but more dense than linear PCL at the same molecular weight. Again, this is expected since the hyperbranched molecule contains a core that is a mixture of both linear and branched monomers and hence will be far less compact than the CCS microgel. A cartoon outlining the various cross-link densities based on the MALLS data is shown graphically in Figure 8 to aid interpretation.

These data suggest that our methodology can be used to synthesize polymers of varying cross-link density in the degradable core, while being able to maintain the nanoparticle structure and prevent macrogelation.

CONCLUSION

Two methodologies have been described for the synthesis of biodegradable core−shell polymers. These were based on degradable cores with varying cross-link densities. In both cases, the shell of the particles was synthesized using RAFT polymerization of DMAEMA—a water-soluble polymer. The molecular characteristics of the polymers were characterized by GPC-MALLS and NMR spectroscopy, and the morphological properties of the materials were investigated by DLS and TEM. A comparison of the hyperbranched methodology and the CCS methodology using GPC-MALLS qualitatively demonstrated that the polymeric chains of the CCS particle were much more densely packed than the hyperbranched molecule. Accelerated degradation on the hyperbranched materials showed that the core underwent facile degradation to a point at which only the water-soluble arms remained. This suggests that they should be of interested in the manufacture of controlled release drug delivery systems. In this case, by varying the size and cross-link density of the core by choice of the synthetic route and the BOD:ε-caprolactone ratio, the degradation time could be tuned to suit the needs of a proposed application. Therefore, these particles would show great potential for use in drug delivery, and future work will involve investigation into the degradation rate of the particles having a range of cross-link densities—from loosely branched to microgels.

ASSOCIATED CONTENT

Supporting Information. ^{1}H NMR spectrum of hyperbranched poly(CL-*co*-BOD)−(DMAEMA) before and after hydrolysis; solid state ^{13}C NMR spectrum of CCS BOD-*b*-DMAEMA. This material is available free of charge via the Internet at http://pubs.acs.org.

AUTHOR INFORMATION

Corresponding Author

*E-mail k.thurecht@uq.edu.au; Tel +44 (0)115 951 3486; Fax +44 (0)115 951 3058.

ACKNOWLEDGMENT

K.J.T. acknowledges the Australian Research Council (DP0880032), The University of Queensland, and the Australian Institute for Bioengineering and Nanotechnology (AIBN) for funding. We acknowledge Dr. Lauren Butler and the Australian National Fabrication Facility.

REFERENCES

(1) Costello, P. A.; Martin, I. K.; Slark, A. T.; Sherrington, D. C.; Titterton, A. *Polymer* **2002**, *43* (2), 245–254.

(2) Hult, A.; Johansson, M.; Malmstrom, E. Hyperbranched polymers. In *Branched Polymers II*; Springer-Verlag: Berlin, 1999; Vol. 143, pp 1−34.

(3) Hedrick, J. L.; Trollsas, M.; Hawker, C. J.; Atthoff, B.; Claesson, H.; Heise, A.; Miller, R. D.; Mecerreyes, D.; Jerome, R.; Dubois, P. *Macromolecules* **1998**, *31* (25), 8691–8705.

(4) Rimmer, S.; England, R. M. *Polym. Chem.* **2010**, *1* (10), 1533–1544.

(5) Qiao, G. G.; Connal, L. A.; Wiltshire, J. T. Porous polymeric materials and polymer particles for preparation thereof. 2006-AU1645; 2007051252, 20061103, 2007.

(6) Wiltshire, J. T.; Qiao, G. G. *Macromolecules* **2008**, *41* (3), 623–631.
(7) Pounder, R. J.; Dove, A. P. *Polym. Chem.* **2010**, *1* (3), 260–271.
(8) Platel, R. H.; Hodgson, L. M.; Williams, C. K. *Polym. Rev.* **2008**, *48* (1), 11–63.
(9) Place, E. S.; George, J. H.; Williams, C. K.; Stevens, M. M. *Chem. Soc. Rev.* **2009**, *38* (4), 1139–1151.
(10) Wiltshire, J. T.; Qiao, G. G. *Macromolecules* **2006**, *39* (26), 9018–9027.
(11) Chiefari, J.; Chong, Y. K.; Ercole, F.; Krstina, J.; Jeffery, J.; Le, T. P. T.; Mayadunne, R. T. A.; Meijs, G. F.; Moad, C. L.; Moad, G.; Rizzardo, E.; Thang, S. H. *Macromolecules* **1998**, *31* (16), 5559–5562.
(12) Wiltshire, J. T.; Qiao, G. G. *Macromolecules* **2006**, *39* (13), 4282–4285.
(13) Konkolewicz, D.; Gray-Weale, A.; Perrier, S. *Macromol. Theory Simul.* **2010**, *19* (5), 219–227.
(14) Liu, B.; Kazlauciunas, A.; Guthrie, J. T.; Perrier, S. *Polymer* **2005**, *46* (17), 6293–6299.
(15) Liu, B.; Kazlauciunas, A.; Guthrie, J. T.; Perrier, S. *Macromolecules* **2005**, *38* (6), 2131–2136.
(16) Semsarilar, M.; Ladmiral, V.; Perrier, S. *Macromolecules* **2010**, *43* (3), 1438–1443.
(17) Matyjaszewski, K. *Polym. Mater. Sci. Eng.* **2001**, *84*, 363–364.
(18) Tsarevsky, N. V.; Huang, J.; Matyjaszewski, K. *J. Polym. Sci., Part A: Polym. Chem.* **2009**, *47* (24), 6839–6851.
(19) Yan, D.; Mueller, A. H. E.; Matyjaszewski, K. *Macromolecules* **1997**, *30* (23), 7024–7033.
(20) Bannister, I.; Billingham, N. C.; Armes, S. P. *Soft Matter* **2009**, *5* (18), 3495–3504.
(21) Isaure, F.; Cormack, P. A. G.; Graham, S.; Sherrington, D. C.; Armes, S. P.; Butun, V. *Chem. Commun.* **2004**, *9*, 1138–1139.
(22) Rosselgong, J.; Armes, S. P.; Barton, W.; Price, D. *Macromolecules* **2009**, *42* (16), 5919–5924.
(23) Rosselgong, J.; Armes, S. P.; Barton, W. R. S.; Price, D. *Macromolecules* **2010**, *43* (5), 2145–2156.
(24) Chang, C.; Wei, H.; Quan, C.-Y.; Li, Y.-Y.; Liu, J.; Wang, Z.-C.; Cheng, S.-X.; Zhang, X.-Z.; Zhuo, R.-X. *J. Polym. Sci., Part A: Polym. Chem.* **2008**, *46* (9), 3048–3057.
(25) Saeed, A. O.; Dey, S.; Howdle, S. M.; Thurecht, K. J.; Alexander, C. *J. Mater. Chem.* **2009**, *19* (26), 4529–4535.
(26) You, Y.; Hong, C.; Wang, W.; Lu, W.; Pan, C. *Macromolecules* **2004**, *37* (26), 9761–9767.
(27) Zeng, F. Q.; Shen, Y. Q.; Zhu, S. P. *Macromol. Rapid Commun.* **2002**, *23* (18), 1113–1117.
(28) Matyjaszewski, K.; Xia, J. H. *Chem. Rev.* **2001**, *101* (9), 2921–2990.
(29) Gao, H. F.; Matyjaszewski, K. *Macromolecules* **2008**, *41* (12), 4250–4257.
(30) Amsden, B. G.; Tse, M. Y.; Turner, N. D.; Knight, D. K.; Pang, S. C. *Biomacromolecules* **2006**, *7* (1), 365–372.